



## Communication

# Noncentrosymmetric $K_2Mn_3(SO_4)_3F_2 \cdot 4H_2O$ and $Rb_2Mn_3(SO_4)_3F_2 \cdot 2H_2O$ with *pseudo*-KTP structures



Yang Zhou<sup>a</sup>, Yanqiang Li<sup>b</sup>, Qingran Ding<sup>b</sup>, Youchao Liu<sup>b</sup>, Yangxin Chen<sup>b</sup>, Xitao Liu<sup>b,c</sup>, Xiaoying Huang<sup>b</sup>, Lina Li<sup>b,c</sup>, Sangen Zhao<sup>b,c,\*</sup>, Junhua Luo<sup>b,c,\*</sup>

<sup>a</sup> College of Chemistry and Materials Science, Fujian Normal University, Fuzhou 350007, China

<sup>b</sup> State Key Laboratory of Structural Chemistry, Fujian Institute of Research on the Structure of Matter, Chinese Academy of Sciences, Fuzhou 350002, China

<sup>c</sup> Fujian Science & Technology Innovation Laboratory for Optoelectronic Information of China, Fuzhou 350108, China

## ARTICLE INFO

## Article history:

Received 28 September 2020

Received in revised form 21 October 2020

Accepted 5 November 2020

Available online 6 November 2020

## Keywords:

Sulfate

Second harmonic generation

Crystal structure

X-ray diffraction

Thermogravimetric analysis

## ABSTRACT

Two fluoride sulfates,  $K_2Mn_3(SO_4)_3F_2 \cdot 4H_2O$  (**I**) and  $Rb_2Mn_3(SO_4)_3F_2 \cdot 2H_2O$  (**II**) are obtained by water solution method. Single-crystal X-ray diffraction analysis indicated that they crystallize in space groups of  $Cmc2_1$ . Their structures feature a *pseudo*-KTP structure consisting of interconnecting  $[Mn_3(SO_4)_3F_2(H_2O)_2]_\infty$  layers, which are further packing along the *a* axis with alkali metal cations balancing the charges. The structure relationships between the two compounds are discussed. Second-harmonic generation measurements manifest that **I** and **II** have similar second-harmonic generation responses of about 0.2 and 0.25 times that of  $KH_2PO_4$ .

© 2020 Chinese Chemical Society and Institute of Materia Medica, Chinese Academy of Medical Sciences. Published by Elsevier B.V. All rights reserved.

Nonlinear optical (NLO) materials are technically importance in producing coherent light sources [1–8]. On the one hand, the NLO materials must meet the crystallographically non-centrosymmetric (NCS). On the other hand, the crystal must satisfy several fundamental requirements such as a wide transparent region, relatively large SHG response, and sufficient birefringence from the viewpoint of optics [9]. Over the past decades, a series of notable NLO crystals have been discovered and used, including  $\beta$ -BaB<sub>2</sub>O<sub>4</sub> [10], LiB<sub>3</sub>O<sub>5</sub> [11], CsLiB<sub>6</sub>O<sub>10</sub> [12,13], KBe<sub>2</sub>B<sub>2</sub>O<sub>6</sub>F<sub>2</sub> [14] and KTiOPO<sub>4</sub> (KTP) [15]. With the rapid development of scientific and technical applications, the search for new NLO materials is still of current academic and commercial interests.

In recent years, several chemical systems of NLO materials have been reported. In terms of borates, notable examples include NaSr<sub>3</sub>Be<sub>3</sub>B<sub>3</sub>O<sub>9</sub>F<sub>4</sub> [16], Na<sub>2</sub>CsBe<sub>6</sub>B<sub>5</sub>O<sub>15</sub> [17], Cd<sub>4</sub>BiO(BO<sub>3</sub>)<sub>3</sub> [18], Pb<sub>2</sub>Ba<sub>3</sub>(BO<sub>3</sub>)<sub>3</sub>Cl [19], as well as Li<sub>4</sub>Sr(BO<sub>3</sub>)<sub>2</sub> [20], Rb<sub>3</sub>Al<sub>3</sub>B<sub>3</sub>O<sub>10</sub>F [21], and K<sub>3</sub>Ba<sub>3</sub>Li<sub>2</sub>Al<sub>4</sub>B<sub>6</sub>O<sub>20</sub>F [22] recently reported by our group. Moreover, there are many carbonates (e.g., ABCO<sub>3</sub>F (A = K, Rb, Cs; B = Ca, Sr, Ba) [23], KMgCO<sub>3</sub>F [24], CsPbCO<sub>3</sub>F [25]), nitrates (e.g., Bi<sub>3</sub>TeO<sub>6</sub>OH(NO<sub>3</sub>)<sub>2</sub> [26], Pb<sub>2</sub>(BO<sub>3</sub>)(NO<sub>3</sub>) [27], Sr<sub>2</sub>(OH)<sub>3</sub>NO<sub>3</sub> [28]), phosphates (e.g., Ba<sub>3</sub>P<sub>3</sub>O<sub>10</sub>X (X = Cl, Br) [29], RbBa<sub>2</sub>(PO<sub>3</sub>)<sub>5</sub> [30],

RbNaMgP<sub>2</sub>O<sub>7</sub> [31]) have been obtained. However, there are fewer reports on sulfate-based NLO materials. One of the main reasons is that sulfates tend to decomposing and releasing SO<sub>3</sub> gas at high temperature, making it difficult to grow bulk crystals by the popular high-temperature molten techniques. Recently, two deep-UV NLO sulfates NH<sub>4</sub>NaLi<sub>2</sub>(SO<sub>4</sub>)<sub>2</sub> and (NH<sub>4</sub>)<sub>2</sub>Na<sub>3</sub>Li<sub>9</sub>(SO<sub>4</sub>)<sub>7</sub> were reported by our group [32], more importantly, they are facile for the crystal growth by a water solution method. Both sulfates are phase-matchable and revealed evident second-harmonic generation (SHG) (1.1 × KH<sub>2</sub>PO<sub>4</sub> (KDP) and 0.5 × KDP), respectively. Furthermore, due to the unsatisfactory arrangement of the two sulfates, there is much room for improving the SHG responses. In addition, Zou and his colleague recently reported a new sulfate CsSbF<sub>2</sub>SO<sub>4</sub>, which exhibits a strong SHG response. CsSbF<sub>2</sub>SO<sub>4</sub> was designed by simultaneously substituting [SbO<sub>4</sub>F<sub>2</sub>]<sup>7-</sup> and [SO<sub>4</sub>]<sup>2-</sup> units for [TiO<sub>6</sub>]<sup>8-</sup> and [PO<sub>4</sub>]<sup>3-</sup> functional groups in KTP, respectively [33]. In this work, two NCS fluoride sulfates,  $K_2Mn_3(SO_4)_3F_2 \cdot 4H_2O$  (**I**) and  $Rb_2Mn_3(SO_4)_3F_2 \cdot 2H_2O$  (**II**) were successfully synthesized by a facile water solution method. The two compounds feature *pseudo*-KTP structures and are NLO-active.

Single crystals of **I** and **II** were obtained *via* water solution. **I** and **II** were prepared through the three steps, which are as follows: (i) The KF or RbF and MnSO<sub>4</sub>·H<sub>2</sub>O of stoichiometric ratio were dissolved in deionized water, respectively, and finally the completely dissolved solution were obtained, (ii) heating the mixture at about 343 K under stirring for 1–2 h, (iii) evaporating

\* Corresponding authors at: State Key Laboratory of Structural Chemistry, Fujian Institute of Research on the Structure of Matter, Chinese Academy of Sciences, Fuzhou 350002, China.

E-mail addresses: zhaosangen@fjirsm.ac.cn (S. Zhao), jhluo@fjirsm.ac.cn (J. Luo).

the mixture at 333 K. Light pink single crystals were obtained. Their crystal structures were determined by single-crystal X-ray diffraction (XRD) (detailed descriptions are listed in Tables S1–S4 in Supporting information). Their powder XRD patterns were consistent with the simulated ones determined from the single-crystal XRD analysis (Fig. S1 in Supporting information). The Energy Disperse Spectroscopy results (Fig. S2 in Supporting information) confirmed the existence of F element in the two compounds.

**I** and **II** crystallize in the same NCS space group  $Cmc2_1$  with similar crystal structures. Hence, the structure of **I** will be illuminated in detail as a representative. There are two crystallographically unique manganese atoms, *i.e.*, Mn1 and Mn2 and two crystallographically unique sulfur atoms, *i.e.*, S1 and S2 in the structure of **I**. The Mn1 atom is attached to two fluorine atoms and four oxygen atoms to form  $Mn1F_2O_4$  octahedron with Mn1-F distances of 2.103 Å and 2.143 Å and Mn1-O distances ranging from 2.137(3) Å to 2.266(4) Å. The Mn2 atom is attached to two fluorine atoms, three oxygen atoms and one water molecule to form  $Mn2F_2O_3(H_2O)$  octahedron with the Mn2-F distances of 2.125(2) Å and 2.199(2) Å and Mn2-O distances ranging from 2.127(3) Å to 2.185(3) Å. The sulfur atoms coordinate with four oxygen atoms to form a  $SO_4$  tetrahedron with the S1–O distances ranging from 1.456(4) Å to 1.503(4) Å and S2–O distances ranging from 1.456(3) Å to 1.482(3) Å.  $Mn1O_4F_2$  and  $Mn2O_3F_2(H_2O)$  octahedra connected with each other *via* sharing edge and sharing corner to form infinite chains along *c* axis (Fig. 1a), which are further connected with  $SO_4$  tetrahedra to form  $[Mn_3(SO_4)_3F_2(H_2O)_2]_\infty$  layers in the *bc* plane (Fig. 1b and Fig. S3 in Supporting information for **II**). The charge balancing  $K^+$  cations and the rest water molecules reside between the layers.

From the viewpoint of structural evolution, **I** can be regarded as a derivative of KTP, in which the  $TiO_6$  octahedra and  $PO_4$  tetrahedra are substituted by  $Mn1O_4F_2$  and  $Mn2O_3F_2(H_2O)$  octahedra and  $SO_4$  tetrahedra, respectively (Figs. 1c and d). Different from the three-dimensional framework composed of  $PO_4$  and  $TiO_6$  in KTP, **I** exhibits a layered structure with  $[Mn_3(SO_4)_3F_2(H_2O)_2]_\infty$  layers. Meanwhile, the connection of octahedra is different. In the structure of KTP, the distorted  $TiO_6$  octahedra share their corners through axial oxygen atoms to form infinite chains. In comparison, each  $Mn1O_4F_2$  octahedron is linked to four  $Mn2O_3F_2(H_2O)$  octahedra *via* corner-sharing and two neighboring  $Mn2O_3F_2(H_2O)$  octahedra are connected *via* edge-sharing in the infinite chains of  $[Mn_3O_{10}F_2(H_2O)_2]$  (Fig. S4 in Supporting information).

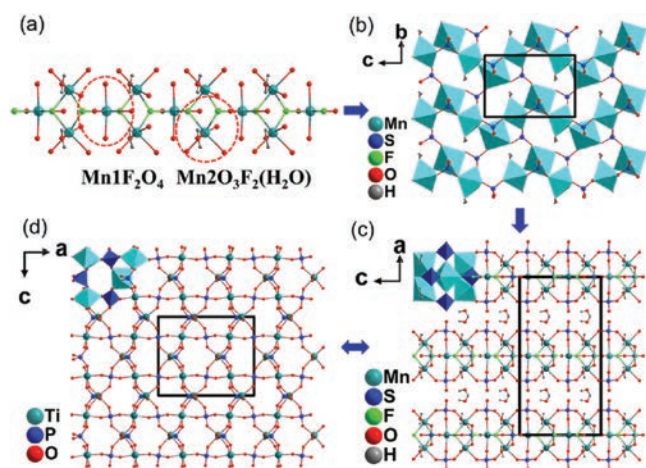


**Fig. 1.** (a)  $[Mn_3O_{10}F_2(H_2O)_2]$  chain. (b)  $[Mn_3(SO_4)_3F_2(H_2O)_2]_\infty$  layer. Structural comparison of (c) **I** and (d)  $KTiOPO_4$ . Dark blue tetrahedra represent  $SO_4$  and light blue octahedra represent  $Mn1O_4F_2$  and  $Mn2O_3F_2(H_2O)$ .

Despite **I** and **II** have different molecular formula, they crystallize in the same space group and have similar layered structures composed of  $Mn1O_4F_2$  and  $Mn2O_3F_2(H_2O)$  octahedra and  $SO_4$  tetrahedra. As shown in Fig. 2a,  $H_2O$  molecular and  $K^+$  cations occupy the interlayer spacing of **I**, whereas only  $Rb^+$  cations reside in the interlayer spacing of **II**. This structural difference is responsible to the different formula. As shown in Fig. 2b, each K atom is coordinated to six oxygen atoms and two water molecular; each Rb atom is coordinated to eight oxygen atoms and only one water molecular. Clearly, the additional water molecular coordinated to the K atoms can provide a larger steric hindrance than oxygen atom, thereby stopping the crystal structure of **I** from collapse, since the K–O distances are evidently shorter than that of Rb–O (Fig. 2b).

The infrared spectra of **I** and **II** are presented in Fig. S5 (Supporting information). The moderate absorption peaks of the two compounds observed at  $3280/1653\text{ cm}^{-1}$  and  $3462/1642\text{ cm}^{-1}$  are attributable to O–H stretching and bending vibrations. Due to the interconnection of the distorted  $Mn1O_4F_2$  and  $Mn2O_3F_2(H_2O)$  octahedral units, the  $SO_4^{2-}$  tetrahedra are very slightly asymmetric, these differential bond lengths in  $SO_4^{2-}$  tetrahedra trigger the degeneration of all stretching and bending vibrational peaks [34]. The signature peaks at lower wavenumbers corresponds to the  $SO_4^{2-}$  building blocks. The peaks at  $1143/1081\text{ cm}^{-1}$  and  $1199/1106\text{ cm}^{-1}$  correspond to  $SO_4^{2-}$  asymmetric stretching vibrations. The peaks at  $979\text{ cm}^{-1}$  and  $1000\text{ cm}^{-1}$  correspond to  $SO_4^{2-}$  symmetric stretching vibrations and the peaks at  $653/612\text{ cm}^{-1}$  and  $697/616\text{ cm}^{-1}$  correspond to  $SO_4^{2-}$  asymmetric bending vibrations [35].

Fig. 3 shows the thermogravimetric analysis curve of **I** and **II**. The result of the test indicated that **I** and **II** gradually lost weight starting from about 377 K and 473 K, the weight losses of 11.2% for **I** and 5.4% for **II**, respectively. Obviously, more crystal water in **I** is the reason for the obvious difference in weight loss between the two compounds. After heating to 873 K in the programmable furnace, the residues of **I** and **II** were  $K_2Mn_2(SO_4)_3$  and  $Rb_2Mn_2(SO_4)_3$ , respectively. They were confirmed by the powder XRD analysis (Fig. S6 in Supporting information). The powder SHG measurements (Fig. 4a) reveal that **I** and **II** exhibit SHG intensities of about 0.2 and  $0.25 \times KDP$  respectively. The SHG tests further confirm the NCS structures of the titled compounds. Based on the anionic group theory, the traditional studies on NLO materials

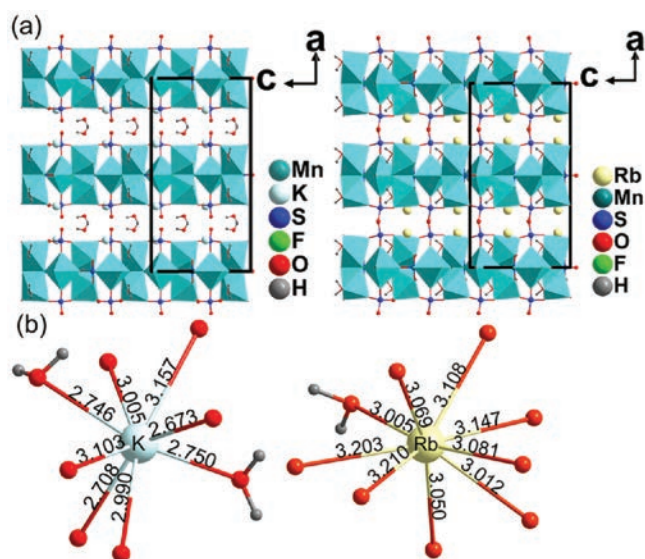


**Fig. 2.** (a) Structural comparison of **I** and **II**. (b) The coordination environment of the alkali atoms.

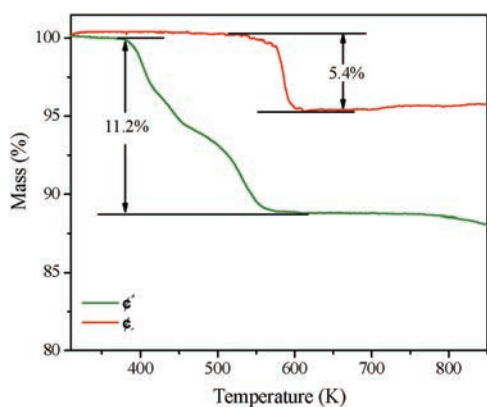


Fig. 3. Thermogravimetric analysis of **I** and **II**.

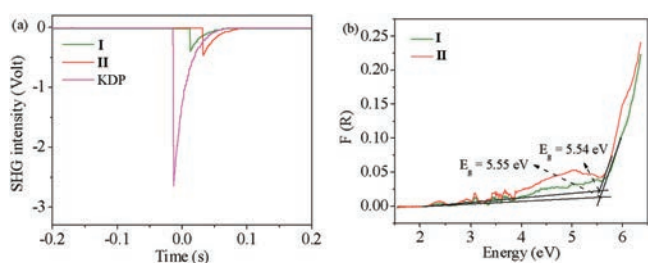


Fig. 4. (a) Comparison on SHG signals for **I**, **II** and KDP. (b) Diffuse reflectance absorption curve of **I** and **II**.

mainly focus on the  $\pi$ -conjugated system, such as  $[\text{BO}_3]^{3-}$ ,  $[\text{CO}_3]^{3-}$  and  $[\text{NO}_3]^{3-}$ , which feature triangular planar geometry. In comparison, sulfates are analogous to phosphates, the microscopic second-order nonlinear susceptibility of the  $\text{SO}_4$  and  $\text{PO}_4$  units are one order of magnitude smaller than that of the planar B–O groups,  $\text{BO}_3$  and  $\text{B}_3\text{O}_6$ . As such, the SHG coefficients of sulfates and phosphates are relatively small [36]. Theoretical calculations on the relationships between the crystal structures and SHG responses will be carried out in the future. The UV–vis near-infrared diffuse reflectance spectrum of **I** and **II** are shown in Fig. 4b. The powders measurements indicate that **I** and **II** display the optical band gap of 5.54 eV and 5.55 eV, respectively. It suggesting that **I** and **II** are broad-band gap materials. (Fig. 4b).

In summary, we have successfully synthesized two new NCS fluoride sulfates by the water solution method, **I** and **II**. Despite the two sulfates have different molecular formula, they crystallize in the same space group and have similar *pseudo*-KTP layered structures. It can be speculated that the steric hindrance of the additional water molecular in comparison with oxygen atom coordinated to the K atoms can prevent the crystal structure of **I** from collapse. In addition, they exhibit relatively weak SHG responses of about 0.2 and  $0.25 \times$  KDP, respectively, which further confirmed that they are NCS. This work enriches the structure chemistry of sulfates.

## Declaration of competing interest

The authors report no declarations of interest.

## Acknowledgments

This work is financially supported by the National Natural Science Foundation of China (Nos. 21833010, 21525104, 21971238, 61975207, 21921001), the Key Research Program of Frontier Sciences of the Chinese Academy of Sciences (No. ZDBS-LY-SLH024), Key Laboratory of Functional Crystals and Laser Technology, TIPC, CAS (No. FCLT 202003), as well as Key Laboratory of New Processing Technology for Nonferrous Metal & Materials, Ministry of Education/Guangxi Key Laboratory of Optical and Electronic Materials and Devices (No. 20KF-11).

## Appendix A. Supplementary data

Supplementary material related to this article can be found, in the online version, at doi:<https://doi.org/10.1016/j.ccl.2020.11.014>.

## References

- [1] S.P. Guo, Y. Chi, G.C. Guo, *Coord. Chem. Rev.* 335 (2017) 44–57.
- [2] Z.G. Xia, K.R. Poeppelmeier, *Acc. Chem. Res.* 50 (2017) 1222–1230.
- [3] B.B. Zhang, G.Q. Shi, Z. Yang, F.F. Zhang, S.L. Pan, *Angew. Chem. Int. Ed.* 56 (2017) 3916–3919.
- [4] G.Q. Shi, Y. Wang, F.F. Zhang, B.B. Zhang, K.R. Poeppelmeier, *J. Am. Chem. Soc.* 139 (2017) 10645–10648.
- [5] M. Mutailipu, M. Zhang, H.P. Wu, et al., *Nat. Commun.* 9 (2018) 3089.
- [6] K.M. Ok, *Acc. Chem. Res.* 49 (2016) 2774–2785.
- [7] G.H. Zou, C.S. Lin, H. Jo, et al., *Angew. Chem. Int. Ed.* 55 (2016) 12078–12082.
- [8] S.P. Guo, Y. Chi, H.G. Xue, *Angew. Chem. Int. Ed.* 57 (2018) 11540–11543.
- [9] P. Becker, *Adv. Mater.* 10 (1998) 979.
- [10] C.T. Chen, B. C. W, A.D. Jiang, G.M. You, *Sci. Sin. Ser. B* 28 (1985) 235–243.
- [11] C.T. Chen, Y.C. Wu, A.D. Jiang, et al., *J. Opt. Soc. Am. B* 6 (1989) 616–621.
- [12] T. Sasaki, I. Kuroda, S. Nakajima, et al., *Appl. Phys. Lett.* 67 (1995) 1818–1820.
- [13] J.M. Tu, D.A. Keszler, *Mater. Res. Bull.* 30 (1995) 209–215.
- [14] L.F. Mei, Y.B. Wang, C.T. Chen, B.C. Wu, *J. Appl. Phys.* 74 (1993) 7014.
- [15] J.D. Bierlein, H. Vanherzeele, *J. Opt. Soc. Am. B: Opt. Phys.* 6 (1989) 622–633.
- [16] D. Cyranoski, *Nature* 457 (2009) 953–956.
- [17] S.C. Wang, N. Ye, *J. Am. Chem. Soc.* 133 (2011) 11458–11461.
- [18] W.L. Zhang, W.D. Cheng, H. Zhang, et al., *J. Am. Chem. Soc.* 132 (2010) 1508–1509.
- [19] X.Y. Dong, Q. Jing, Y.J. Shi, et al., *J. Am. Chem. Soc.* 137 (2015) 9417–9422.
- [20] S.G. Zhao, P.F. Gong, L. Bai, et al., *Nat. Commun.* 5 (2014) 4019.
- [21] S.G. Zhao, P.F. Gong, S.Y. Luo, et al., *J. Am. Chem. Soc.* 137 (2015) 2207–2210.
- [22] S.G. Zhao, L. Kang, Y.G. Shen, et al., *J. Am. Chem. Soc.* 138 (2016) 2961–2964.
- [23] G.H. Zou, N. Ye, L. Huang, X.S. Lin, *J. Am. Chem. Soc.* 133 (2011) 20001–20007.
- [24] T.T. Tran, J. Young, J.M. Rondinelli, P.S. Halasyamani, *J. Am. Chem. Soc.* 139 (2017) 1285–1295.
- [25] G.H. Zou, L. Huang, N. Ye, et al., *J. Am. Chem. Soc.* 135 (2013) 18560–18566.
- [26] S.G. Zhao, Y. Yang, Y.G. Shen, et al., *Angew. Chem. Int. Ed.* 56 (2017) 540–544.
- [27] J.L. Song, C.L. Hu, X. Xu, F. Kong, J.G. Mao, *Angew. Chem. Int. Ed.* 54 (2015) 3679–3682.
- [28] L. Huang, G.H. Zou, H.Q. Cai, *J. Mater. Chem. C* 3 (2015) 5268–5274.
- [29] P. Yu, L.M. Wu, L.J. Zhou, L. Chen, *J. Am. Chem. Soc.* 136 (2014) 480–487.
- [30] S.G. Zhao, P.F. Gong, S.Y. Luo, et al., *J. Am. Chem. Soc.* 136 (2014) 8560–8563.
- [31] S.G. Zhao, X.Y. Yang, Y. Yang, et al., *J. Am. Chem. Soc.* 140 (2018) 1592–1595.
- [32] Y.Q. Li, F. Liang, S.G. Zhao, et al., *J. Am. Chem. Soc.* 141 (2019) 3833–3837.
- [33] X.H. Dong, L. Huang, C.F. Hu, et al., *Angew. Chem., Int. Ed.* 58 (2019) 6528–6534.
- [34] K. Nakamoto, *Infrared and Raman Spectra of Inorganic and Coordination Compounds*, Wiley, New York, 1986.
- [35] P. Barpanda, C.D. Ling, G. Oyama, A. Yamada, *Acta Crystallogr. B: Struct. Sci. Cryst. Eng. Mater.* 69 (2013) 584–588.
- [36] L. Li, Y. Wang, B.H. Lei, et al., *J. Am. Chem. Soc.* 138 (2016) 9101–9104.